Electronic Supplementary Material (ESI) for Lab on a Chip.

Supplementary Information

Natural gas vaporization in a nanoscale throat connected model of shale: Multi-scale, Multi-component and Multi-phase

Arnav Jatukaran, [a] Junjie Zhong, [a] Ali Abedini, [b] Atena Sherbatian, [a] Yinuo Zhao, [c] Zhehui Jin, [c] Farshid Mostowfi, [d] and David Sinton *[a]

[a] Department of Mechanical and Industrial Engineering, University of Toronto, Toronto, Ontario M5S 3G8, Canada

[b] Interface Fluidics Limited, Edmonton, AB T6G 1V6, Canada

[c] Department of Civil and Environmental Engineering, University of Alberta, 9211 - 116 Street NW, Edmonton, Alberta T6G 1H9, Canada

[d] Schlumberger-Doll Research, Cambridge, Massachusetts 02139, United States

Contents

Section 1: Nanomodel Fabrication and Experimental Set-up

Each fabricated chip contained two nanomodels (2 mm × 1.5 mm) placed perpendicular to the 20 µm deep service microchannel that had a drilled inlet hole for the fluid sample injection. A schematic of key fabrication steps is shown in Fig. 1. To fabricate the device, 1) a 200-nm thick film of silicon nitride was first deposited onto the bare silicon wafer (4-inch diameter, 1-mm thick silicon wafer) using low pressure chemical vapor deposition (Expertech CTR-200 LPCVD). 2) Following this, ZEP-520A e-beam resist was spin-coated onto the wafer and the 5-nm pore network was patterned using electron-beam lithography (Vistec EBPG 5000+ Electron Beam Lithography System). 3) Deep-reactive-ion-etching (DRIE, Oxford Instruments PlasmaPro Estrelas100 DRIE System) was used to etch the 5-nm pore network pattern resulting in the 5-nm deep and ~100 nm-wide network of channels. 4) The substrate was then cleaned in a Piranha solution (H_2SO_4:H_2O_2 = 3:1) for 1 hour to remove the photoresist. 5) Following this, the large nanopore pattern was written on a photo mask (Heidelberg µPG 501) and transferred onto the wafer coated with S1818 photoresist using UV lithography (Suss MicroTec MA6 Mask Aligner). The pattern was then etched using DRIE resulting in the ~82 nm deep large nanopore features. 6) The substrate was then cleaned in Piranha solution for 1 hour. 7) Following this, the service microchannel pattern was written on a photo mask and transferred onto the wafer coated with AZ9260 photoresist using UV lithography. The service microchannels were then etched using DRIE. A 400 µm deep channel was also etched 1 mm above the location of the nanomodel into which thermocouples were inserted to determine experimental temperature following experiment. Inlet holes were then drilled through the silicon wafer. 8) After cleaning the wafer and a 2-mm thick Borosilicate glass slide in Piranha solution for 1 hour, the two were anodically bonded at 673 K, 10^{-3} Pa and 100 V for approximately 5 minutes (AML AWB-04 Aligner Wafer Bonder). 9) The bonded device was then diced into the desired shape to fit the experimental set-up (Disco DAD3220 Automatic Dicing Saw). Table S1 shows the depths and widths of the 5-nm throat network and the large nanopores.

Table S1 Summary of pore size dimensions

Pore type	Height (nm)	Average Width (nm)
Large pores	82.2	6000
5-nm throat network	5.5	100

The nanofluidic device was mounted on a custom-built high-pressure, high-temperature manifold and connected to the experimental set-up shown in Fig. 2. All components of the set-up (tubing, piston cylinder, valves and manifold) were thoroughly cleaned using DI water and dried using an air gun. The nanofluidic chip was placed under an optical microscope (Leica DM 2700M) with a 10X objective lens, allowing the visualization of vaporization in two different nanoporous media simultaneously. Vaporization was recorded using a camera (Leica DMC 2900).

Temperature was controlled by placing a copper block connected to an electric heater (accuracy ± 0.1 ºC) below the location of the nanomodel. The experimental temperature (T) was determined by measuring the temperature close to the nanomodel by inserting a thermocouple in a 400 µm deep channel etched 1-mm above the location of the nanomodel. Over the course of the experiment, the temperature variation was approximately ± 0.5 ºC. The hydrocarbon mixture was produced in-lab by combining a mixture of 80% propane and 20% methane (mol. fraction, Praxair Canada) and pentane (Sigma Aldrich) in a piston cylinder in liquid-phase. The final liquid composition was 10% methane, 40% propane and 50% pentane (mol. fractions). Pressure in the chip was controlled using an ISCO pump and measured using a pressure transducer (resolution at 1 kPa).

Prior to running the experiments, the entire system was vacuumed for three hours at 2×10^{-4} kPa (PFPE RV8) to remove residual air from the system. The nanomodel was initially filled with liquid sample at pressures above the bubble point pressure at room temperature (4 MPa). After waiting ~12 hours to reach the compositional equilibrium condition, temperature was increased to the experimental temperature, T, using the electric heater. Experimental temperatures here included 42.5°C, 62.5°C and 82.5°C. After waiting one hour to allow the system to reach thermal equilibrium, pressure was lowered to a target pressure below the bubble point pressure to

observe vaporization. At each temperature, pressure was lowered to 2 MPa and 1 MPa and finally to vacuum. At each increment, the waiting time of 15 minutes was set to observe vaporization.

Section 2: Image Processing

Images were batch processed by first smoothening the images by applying a Gaussian filter operation, followed by thresholding to create a binary image to isolate empty circles (both isolated and vaporized pores). A MATLAB algorithm was then used to count the number of vaporized pores as a function of time. Isolated pores were removed by subtracting each image by a reference image taken with the nanomodel fully saturated with liquid.

Section 3: Porosity and Permeability Calculations

The porosity of the dual-depth nanomodel was determined by first determining the areal porosity of the 5-nm throat to be $\varphi_{throat} =$ 5% and the 100-nm pore to be $\varphi_{pore} =$ 10% using AutoCAD design files. The contribution of the two different pore sizes to the porosity was then determined to be:[1]

$$\varphi = \frac{\frac{H}{h_{throat}}(\varphi_{pore}) + \varphi_{throat}}{H/h_{throat}} \quad (1)$$

Here, H is the height of the larger pores (82 nm) and h_{throat} is the height of the 5-nm pore network (5.5 nm). The dual porosity is then determined to be 10.3%.

The Kozeny equation was used to determine absolute permeability:

$$k = a\left(\frac{\varphi^3 h_{throat}^{\ 2}}{(1-\varphi)^2}\right) \quad (2)$$

Here, a is used to convert m^2 to units of D and has a value of 1.013×10^{12} D/m^2. The permeability is then calculated to be 44 nD.

Section 4: Vaporization Model

MATLAB was used to calculate vaporization dynamics under different pressure/temperature conditions. In the code, a linear array of large 100-nm pore is created that are separated by the

5-nm throats. The vapor transport time in the 5-nm throats is determined by first calculating the vapor transport resistance in the 5-nm throats. The vapor transport resistance, R_V, is comprised of the Knudsen flow resistance and viscous flow resistance components and can be determined as below:[2]

$$R_V = \frac{\rho_l/\rho_g}{\frac{h_{throat}^2}{12u_g} + \frac{2\sqrt{2}h_{throat}}{3\rho_g}\sqrt{\frac{\bar{M}}{\pi RT}}} \quad (3)$$

where ρ_g and ρ_l are the gas and liquid density, h_{throat} is the height of channel in the throat network, u_g is the gas viscosity, $\bar{M}$ is the average molar mass, R is the gas constant and T is the temperature. With regards to mixture parameters, vapor composition was determined using Equation of State (EOS) calculations at the dew point of the initial liquid composition used (0.1/0.4/0.5 mol. fraction of C1/C3/C5). Vapor phase composition was used to determine the average molar mass using mol. fraction of each component, x_i, and molar mass of each component, M_i,:

$$\bar{M} = \sum x_i M_i = x_{C1}M_{C1} + x_{C3}M_{C3} + x_{C5}M_{C5} \quad (4)$$

Liquid density was obtained using EOS at the bubble point of the initial liquid composition. Vapor density was calculated by taking the average of the vapor density at the dew point of the initial liquid composition and vapor density close to the inlet (~ 0 kg/m^3 due to vacuum condition). Vapor viscosity was approximated at the dew point the vapor composition and estimated using REFPROP. Liquid density, vapor density and vapor viscosity were obtained using REFPROP at bulk saturation conditions. A summary of fluid parameters is included in Table S2:

Table S2 Summary of fluid parameters used in the modelling of vaporization dynamics.

Model Case	Superheat, ΔP (MPa)	Vapor composition $C_1/C_3/C_5$ (mol. fraction)	Liquid density, ρ_l (kg/m^3)	Vapor density, ρ_g (kg/m^3)	Vapor viscosity, u_g (Pa.s)

High Superheat	0.76	0.24/0.50/0.26	465.97	12.92	1.01E-05
Medium Superheat	0.44	0.33/0.48/0.19	501.19	8.67	9.94E-06
Low Superheat	0.24	0.43/0.44/0.13	531.55	6.46	9.69E-06

Using Equation (3), the transport time, t_{vap}^{throat}, through the 5-nm throats is determined as below:

$$t_{vap}^{throat} = \frac{R_V L_{throat}^{\ 2}}{2\Delta P} \qquad (5)$$

Here, L_{throat} is the length of the small nanopore network and ΔP is the superheat. The volumetric vapor flow rate in the 5-nm throat, Q_{throat}, is then determined:

$$Q_{throat} = \frac{L_{throat} A_{throat}}{t_{vap}^{throat}} \qquad (6)$$

Here, A_{throat} is the cross-sectional area of a 5-nm throat. At each 100-nm pore location, we also determine the time required to empty the volume held in a large pore through the 5-nm network, t_{vap}^{pore}, by relating the 100-nm pore volume, V_{pore}, and the volumetric vapor flow rate in the 5-nm network, Q_{net}.

$$t_{vap}^{pore} = \frac{V_{pore}}{Q_{net}} \qquad (7)$$

This calculation is repeated for the entire geometry and the cumulative vaporization time (combining 5-nm throat network transport time and 100-nm pore emptying time) is then determined. A schematic of the geometry used in the model is shown in Fig. S1.

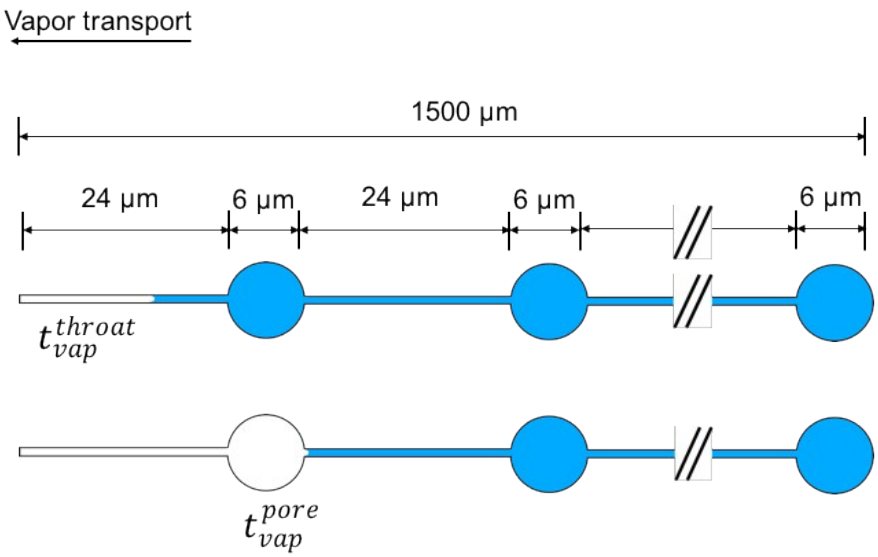

Fig. S1 Simplified geometry used to calculate the vaporization dynamics (top-view). The time taken for vapor flow through the 5-nm throats, t_{vap}^{throat}, is calculated by determining the volumetric flow rate through small pores using a resistance model containing both Knudsen flow resistance and viscous flow resistance contributions. The time taken to transport vapor volume held in a 100-nm pore, t_{vap}^{pore} is calculated by using the 5-nm throats vapor volumetric flow rate and the volume of a 100-nm pore.

Section 5: Filling Model

A similar MATLAB model and geometry as shown in Fig. S1 is used to calculated the expected filling dynamics in the nanomodel. Hagen-Poiseuille is used to determine filling dynamics in the 5-nm throats with a filling time, t_{fill}^{throat}, calculated as:

$$t_{fill}^{throat} = \frac{12 L_{throat}^{2} A_{throat} \mu_l}{P_{fill} h_{throat}^{3} w_{throat}} \quad (8)$$

Here, w_{throat} is the width of the 5-nm throat, respectively, and μ_l is the liquid viscosity. P_{fill} is the filling pressure calculated as the difference between the liquid pressure, P_l and the capillary pressure, P_{cap}, in a 100-nm pore:

$$P_{fill} = P_l - P_{cap} \quad (9)$$

Here, capillary pressure is estimated as:

$$P_{cap} = \frac{2\sigma \cos(\theta)}{H} \quad (10)$$

Where σ is the interfacial tension (~0.006 N/m),[3] θ is the contact angle (assumed to be zero here) and H is the height of 100-nm pore.

Employing a similar algorithm as in Section 4, we use the filling time determined in equation (8) to calculate the time required to fill 100-nm pore. This is done by relating the volume of a 100-nm pore to the volumetric velocity in the 5-nm throat. The calculation results in a step-function with a square-root-of-time dependence on the time. The horizontal steps represent the time necessary to fill a large nanopore with liquid and the vertical jumps represent the relatively fast filling of the 5-nm throat.

We also estimate the pressure drop across the orifice geometry (i.e., the transition between pore throat and the large pore) and find that it is negligible compared to the capillary pressure in the larger nanopores:[4]

$$\Delta P = \frac{1}{2}\rho\left(1-\frac{h^4}{H^4}\right)\left(\frac{V}{CY}\right)^2$$

Where ΔP is the pressure loss for one orifice, ρ is the mixture liquid density, h is the pore throat height (5.5 nm), H is the big pore height (82 nm), V is the flow velocity at dead-end (estimated to be 1.47×10^{-7} m/s), C is the discharge coefficient (here 0.61), and Y is the Expansion coefficient (here 1 for incompressible flow). The calculation result for ΔP is: 1.59×10^{-11} Pa, and the total pressure loss on our chip due to orifice geometry is: 7.95×10^{-10} Pa (considering ~50 large pores if arranged serially as in Fig. S1), which is negligible compared to the capillary pressure in the large nanopore (0.15 MPa).

Section 6: Diffusion Model

To quickly estimate the diffusion effect in the nanomodel, we assume that bulk diffusivity is still applicable at nanoscale for small hydrocarbon molecules (e.g., pentane here). In this case, we can calculate the diffusivity of pentane molecule in the liquid mixture through the Einstein–Smoluchowski relation:

$$D = \frac{k_B T}{6\pi r \eta} \qquad (11)$$

Where k_B is the Boltzmann constant, T is the temperature, r is the molecular radius, η is the fluid dynamic viscosity. For the pentane molecule in the fluid mixture here, $D = 4 \times 10^{-9}$ m²/s.

When considering the geometry of the nanomodel (Fig. S1), the mass transport between the large pores is through the 5-nm pore throat. Therefore, when considering the diffusion between two large pores, the diffusivity is effectively reduced as a function of the cross-sectional area (*A*):

$$D' = D\frac{A_{porethroat}}{A_{largepore}} \quad (12)$$

The diffusion effect within the nanomodel can now be estimated with the Fick's second law:

$$\frac{dc}{dt} = D_{eff}\frac{d^2c}{dx^2} \quad (13)$$

The effective diffusivity D_{eff} equals to D when calculating the diffusion within the pore throat, and equals to D' when calculating the diffusion within the large pore. The numerical solutions are shown in Fig. S2.

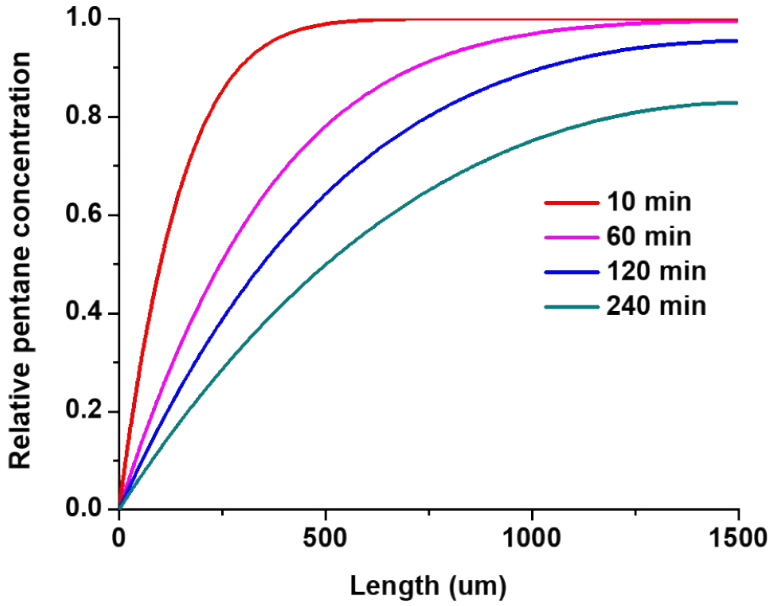

Fig. S2 Pentane relative concentration change along the nanomodel through diffusion at 10 min, 60 min, 120 min and 240 min, from inlet (0 μm) to dead end (1500 μm).

Section 7: Supplementary Data

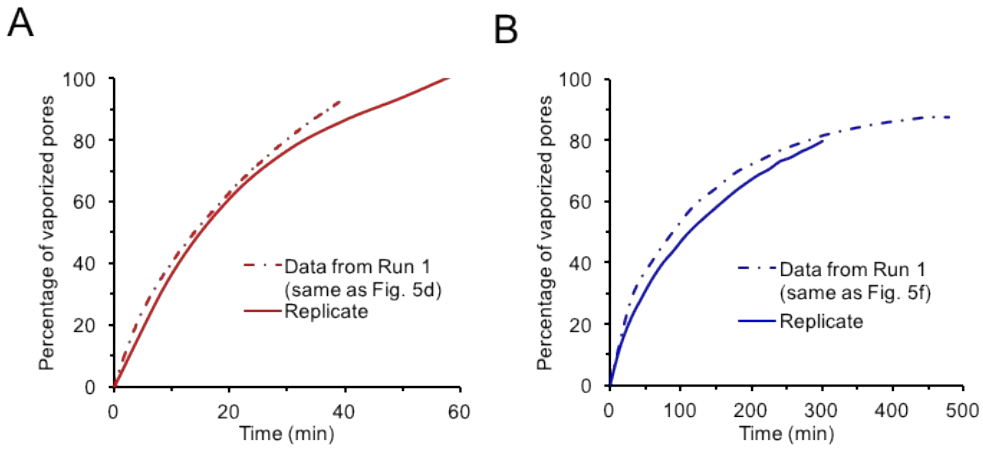

Fig. S3 Vaporization data from replicate experiments shows good agreement. (A) Data for 0.76 MPa superheat and (B) 0.24 MPa superheat. Dashed lines are same as in Fig. 5d and 5f, respectively. Solid lines represent repeat experiment.

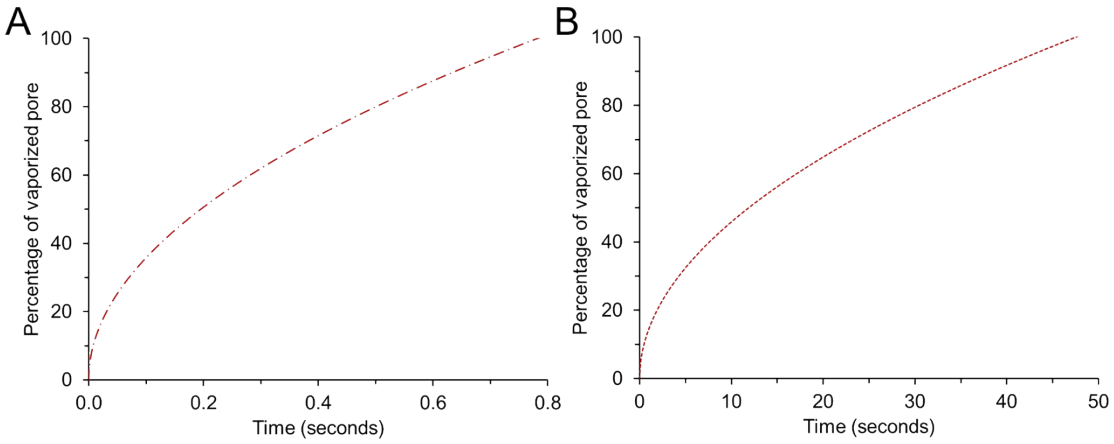

Fig. S4 (A) Calculated vaporization profile for a single, discrete 82-nm deep channel under high-superheat thermodynamic conditions without a gating 5-nm pore network. (B) Calculated vaporization profile for a single, discrete 5.5-nm deep channel under high-superheat thermodynamic conditions

References

1 W. Yun, C. M. Ross, S. Roman and A. R. Kovscek, *Lab Chip*, 2017, **17**, 1462–1474.

2 J. Zhong, S. H. Zandavi, H. Li, B. Bao, A. H. Persad, F. Mostowfi and D. Sinton, *ACS Nano*, 2017, **11**, 304–313.

3 W. D. McCain, *The Properties of Petroleum Fluids*, PennWell Publishing Company, 2nd edn., 1990.

4 R. W. Miller, *Flow Measurement Engineering Handbook*, McGraw-Hill, 3rd edn., 1996.